# Evaluating the Use of a Nonlinear Two-Dimensional Model in Downslope Windstorm Forecasts

LOUISA B. NANCE

*Cooperative Institute for Research in Environmental Sciences, University of Colorado/NOAA/Environmental Technology Laboratory, Boulder, Colorado*

BRADLEY R. COLMAN

*National Weather Service Forecast Office, Seattle, Washington*

(Manuscript received 27 September 1999, in final form 10 July 2000)

ABSTRACT

Severe downslope windstorms are a mesoscale, primarily wintertime, phenomenon that affect regions in the lee of large mountain ranges. The resolution of current weather prediction models is too coarse to explicitly predict downslope windstorms. Hence, additional operational tools are needed for making downslope windstorm forecasts. Current windstorm forecast techniques commonly utilize a tool referred to as a ''decision tree.'' Although decision trees provide valuable guidance, operational forecasters have not found this type of tool to be highly reliable. With recent advances in computer technology, a new type of operational tool is available for forecasting downslope windstorms: two-dimensional, nonlinear, mesoscale numerical models. This study investigates whether this type of model, initialized with upstream profiles taken from operational Eta Model forecasts, can produce accurate downslope windstorm forecasts.

Numerical simulations for high-wind events that affected seven regions in the United States between January 1993 and April 1997 indicate this tool is able to produce lee-slope wind speeds that meet the local peak gust threshold for a High Wind Warning for a majority of those cases where observed winds met this threshold. These simulations were initialized with upstream soundings taken from the 12- and 18-h Eta forecasts valid at the time of each high-wind event. A comparison for one region between the number of events for which High Wind Watches were posted and the number of events for which the two-dimensional model prediction met the peak gust threshold suggests this new tool would be a definite improvement over the current forecast technique. On the other hand, a preliminary test of the model's ability to differentiate between windstorm and nonwindstorm events suggests the false warning rate for this tool may be high. Further testing of this tool is ongoing and will continue through the winter months of 2000/01.

## 1. Introduction

A number of communities located in the lee of mountainous regions of the United States (e.g., Boulder, CO; Juneau, AK; Salt Lake City, UT) experience strong downslope winds that often gust to well above nominal hurricane force (34 m $s^{-1}$). These high-wind events are frequently responsible for considerable property damage and occasionally serious injury or loss of life. The property damage caused by downslope windstorms in the Boulder area alone averaged about $1 million (in 1975 dollars) each year in the early 1970s. Three deaths and more than 50 injuries were connected to downslope windstorms that occurred in the Boulder area between the winter of 1964/65 and the winter of 1976/77 (Bergen and Murphy 1978). Over the past two decades, population densities in the communities affected by these violent windstorms have been on the rise, creating the potential for significantly larger amounts of property damage. An investigation into the social and economic impact of improved windstorm forecasts by Bergen and Murphy (1978) suggests that improving the accuracy of the 1970s windstorm forecasts from 30% to 80% would significantly increase the implementation of a variety of protective actions, which in turn, could lead to a substantial reduction in the amount of property damage and possibly reduce the risk of serious injury.

Downslope windstorms can also create hazardous conditions for various modes of transportation. The clear-air turbulence associated with downslope windstorms presents a hazard to aircraft. For instance, on 9 December 1992, severe turbulence related to a downslope windstorm in Boulder, Colorado, was responsible for an accident in which a DC-8 jet lost an engine and part of a wing, forcing an emergency landing (Ralph et

*Corresponding author address:* Dr. Louisa B. Nance, NOAA/ETL, R/ET7, 325 Broadway, Boulder, CO 80303-3328.
E-mail: lnance@etl.noaa.gov

al. 1997; Clark et al. 2000). The superstructure icing associated with the boratype high-wind events (cold winds) that affect Juneau, Alaska, known locally as the Taku wind, creates hazardous conditions for shipping (Colman and Dierking 1992). By providing more accurate information about local conditions through improved windstorm forecasts, the risk of aircraft and shipping accidents could be substantially reduced.

Observational evidence indicates downslope windstorms occur when there is a strong low-level amplification of a terrain-induced gravity wave (e.g., Lilly and Zipser 1972). Cross-barrier flow at mountaintop level is necessary to generate terrain-induced gravity waves. By compositing upstream profiles, Brinkmann (1974) found that the existence of a stable layer above mountaintop, strong winds at the level of the stable layer, and winds much weaker than the mean in the middle and upper troposphere are favorable for Boulder downslope windstorms. Observational studies for other regions have also found that the existence of a flow reversal in the middle troposphere is favorable for terrain-induced windstorms (e.g., Reed 1981; Smith 1987; Colman and Dierking 1992).

The exact mechanisms through which low-level amplification of terrain-induced gravity waves occurs are not fully understood, but theoretical and numerical modeling studies have revealed three different circumstances for which low-level amplification of a mountain wave can occur: 1) an inversion or stable layer near or slightly above mountaintop, 2) capping by a mean-state critical level, and 3) wave breaking (e.g., Clark and Peltier 1977; Smith 1987; Durran 1986). The critical level for stationary mountain waves generated by steady flow over an elongated mountain ridge is the level at which the cross-barrier flow is zero. Wave breaking occurs in regions where the total cross-barrier flow ($\overline{u} + u'$) goes to zero, so the term wave-induced critical level is often used to describe the level at which a mountain wave breaks. These circumstances induce transitions in the nonlinear mountain wave solution that are qualitatively similar to the transitions that occur in the flow of water over a rock (e.g., Smith 1985; Durran 1986; Durran and Klemp 1987).

The connection between hydraulic theory and the wave amplification process for static stability layering and critical levels in the atmosphere allows one to construct a simple unified model for the creation of high lee-slope velocities in a variety of geophysical flows. This model consists of a two-part amplification process. In the first part of this amplification process, the pressure gradient force in the standing gravity wave dominates the force balance on fluid parcels upstream of the obstacle crest, causing the fluid near the crest to experience a net acceleration. In the second part of this amplification process, which occurs only when the obstacle is sufficiently high, the flow undergoes a transition at the crest such that gravity dominates the force balance on the fluid parcels downstream of the obstacle crest, causing the fluid to continue to accelerate on the lee slope of the obstacle. In hydraulic theory, this two-part amplification is referred to as a transition from subcritical to supercritical flow (Durran 1990).

Although the hydraulic analog provides a simple context for describing the dynamics involved in the generation of a downslope windstorm, it does not provide much practical assistance to operational forecasters. To apply this analog, one must specify an effective depth of the fluid. This depth is determined by the process (wave breaking, static stability layering, or capping by a mean-state critical level) promoting the development of an atmospheric hydraulic jump. Determining which process is promoting this development from knowledge of the upstream environment is oftentimes difficult because the upstream flow can exhibit characteristics conducive to more than one of these processes. Identifying the effective depth is further complicated by the fact that the development of wave breaking can be regulated by subtle features in the upstream flow (Durran 1986). Consequently, the onset and position of breaking waves cannot be predicted without recourse to numerical simulation (Durran and Klemp 1987).

## 2. Current status of downslope windstorm forecasts

With the addition of the Eta Model, the family of weather prediction models run at the National Centers for Environmental Prediction (NCEP) has come a long way toward better resolving mesoscale phenomena, but the current resolution of this mesoscale model (horizontal grid spacing of 32 km) is still too coarse to explicitly predict downslope windstorms. Hence, additional operational tools are still needed for making downslope windstorm forecasts. Current windstorm forecast techniques commonly utilize a tool referred to as a ''decision tree,'' which leads the forecaster in a step-by-step fashion to a prediction for downslope winds in a particular region. A decision tree is developed by cataloging the values of parameters known to be important to low-level wave amplification during past windstorms in a particular region and then identifying the ranges of these parameters that indicate a windstorm threat (Colman and Dierking 1992).

Current downslope windstorm forecasts for Boulder are based on a decision tree developed by J. Brown at the National Oceanic and Atmospheric Administration's (NOAA) Forecast Systems Laboratory (FSL). Brown's decision tree considers the following: 1) the geostrophic winds at 700 and 500 mb, 2) the temperature difference between 500 and 300 mb, and 3) the existence of a cold air mass east of Colorado's Front Range. This information is run through a regression calculation based on Nested Grid Model (NGM) analyses for past Boulder windstorm cases, which yields a probability for high winds in Boulder (Brown 1986; Brown et al. 1992).

The windstorm forecasts for the western slopes of the

Washington Cascades are based on a decision tree developed by the second author at the Seattle National Weather Service Forecast Office (NWSFO). This decision tree attempts to differentiate between the conditions favorable for the development of strong downslope winds and those favorable for the development of gap winds. Colman's decision tree considers the wind speed and direction at 850 mb, the existence of a flow reversal near 700 mb, the presence of a stable layer near mountaintop, and the strength of the pressure gradient across the Cascade Range. Since this particular decision tree is not model specific, the guidance can be applied to the forecaster's model of choice.

Operational forecasts for the Taku wind in Alaska use a relatively simple program that evaluates either Eta or NGM sounding data. This program assigns weights for given rules and conditions based on criteria identified in the observational study by Colman and Dierking (1992) and then summarizes the mountain wave potential as either ''good,'' ''marginal,'' or ''unlikely.''

Although decision trees provide valuable guidance, operational forecasters have not found this type of tool to be highly reliable when it comes to forecasting downslope windstorms. For example, a recent preliminary study of Boulder wind events for the winters of 1993/94 and 1994/95 found that only 40% of the High Wind Watches issued by the Denver NWSFO for downslope wind events verified (E. Thaler, Denver NWSFO, 1995, personal communication) This estimate suggests the current accuracy of windstorm forecasts may be slightly higher than that in the 1970s, but the results of Bergen and Murphy's (1978) study indicate this accuracy needs to be increased to at least 80% before a significant increase in the implementation of protective actions would occur.

## 3. Description of the new forecast tool

Many of the recent theoretical advances in the understanding of downslope windstorms have stemmed from studies using two-dimensional, nonlinear, numerical models to investigate how changes in the upstream conditions will affect airflow over terrain. The initial success of a simple linear, two-dimensional, steady-state, multilayer model proposed by Klemp and Lilly (1975) suggests that two-dimensional models may be able to predict strong downslope wind events from knowledge of the upstream environment. The idealized numerical modeling study by Durran (1986) highlights the importance of nonlinear effects in the low-level amplification of a mountain wave. In the past, the nonlinear models used in the theoretical studies of downslope windstorms have been too computationally intensive to be run locally in real time. With recent advances in computer technology and the recent hardware upgrade at National Weather Service forecast offices, the two-dimensional, nonlinear, mesoscale numerical models used in theoretical studies of downslope windstorms can now be run in real time on a workstation in the local forecast office.

This study investigates whether this type of numerical model, initialized with a representative terrain profile and an upstream atmospheric profile taken from operational Eta forecast grids, can produce accurate downslope windstorm forecasts. Unlike the decision trees currently used in operational forecasting, this type of tool could be applied to a number of locations with only minor modifications to accommodate differences in the local terrain and the location of the upstream profile. More importantly, this type of forecast tool is able to account for the complex nonlinear dynamics associated with this mesoscale phenomenon.

The two-dimensional nature of the forecast tool considered in this study precludes the influence of three-dimensional effects, which may, under certain conditions, play an important role in determining the structure of the mountain wave and the strength of the lee-slope flow. Several regional groups are exploring the real-time use of high-resolution three-dimensional numerical models (Mass and Kuo 1998). Early results are very promising and it is likely that further advances in the forecasting of wave-induced windstorms will occur as a result of these three-dimensional models becoming operationally available. Unfortunately, such capabilities are currently not available in all forecast offices. One potential advantage of the two-dimensional framework is the simplification of the problem, which aids the forecaster's ability to associate the output with a particular phenomenonological conceptual model. Whereas, forecasters in regions where three-dimensional guidance is currently available can, at times, find the flow patterns difficult to interpret due to their complexity.

As NWP transitions to an era of readily available real-time, high-resolution guidance, the type of tool considered in this study could become an educational tool. As the authors have already found, forecasters can gain a better understanding of mountain wave dynamics through hands-on experience running a two-dimensional model initialized with a variety of upstream profiles, which can then be applied to the interpretation of complex three-dimensional terrain-induced flow patterns.

The numerical model used in this study is based on the fully compressible model developed by Durran and Klemp (1983). This model is designed to calculate two-dimensional, high Rossby number airflow ($f \rightarrow 0$) over an infinitely long uniform mountain barrier. Open boundary conditions that allow disturbances to propagate out of the domain without generating spurious reflections are imposed at the top and lateral boundaries (Durran et al. 1993; Klemp and Durran 1983). Terrain is incorporated at the lower boundary through the use of a terrain-following coordinate system. A free-slip boundary condition is applied at the surface and the dry physics option is employed in all of the simulations considered in this study.

The version of the model used in this study runs on

an HP 7000 series UNIX workstation, and is equipped with an input interface through which the user specifies the following: the projection angle for the cross-mountain wind component; the representative terrain profile for the local region; and the date and hour of the Eta Model initialization, the forecast hour, and the grid point to be used to obtain an upstream profile. The input interface retrieves vertical profiles of potential temperature ($\theta$), geopotential height, and the components of the horizontal wind vector for the specified time and location. This single upstream profile is used to initialize the two-dimensional model with a horizontally homogeneous, hydrostatically balanced basic state. The two-dimensional model is then integrated to 4 h. The horizontal wind profile and gravitational constant are gradually increased from zero to their specified values over the first 500 and 2000 s, respectively, of the integration to reduce the gravity wave transients generated by this initialization process in the presence of topography. The output fields available at the end of the integration include horizontal velocity ($u$), vertical velocity ($w$), perturbation pressure ($p'$), and $\theta$. An integration time of 4 h was chosen because it is generally sufficient to obtain a mature mountain wave response to the prescribed background conditions. It is important to keep in mind the integration time of the two-dimensional model does not directly correspond to real time. Instead, it should be viewed as spinup time. All of the numerical simulations considered in this study were computed on a domain 20 km deep with a vertical grid spacing of 250 m and a horizontal grid spacing of 2 km. The width of the model domain depended on the horizontal scale of the local terrain.

The surface wind speeds from the Eta Model forecast fields are typically too light, especially inland (Staudenmaier and Mittelstadt 1997). According to linear theory, the amplitude of the gravity wave generated by flow over underlying topography is determined, at least in part, by the surface wind speed, which in turn, suggests that using the Eta Model surface winds to initialize the two-dimensional model would adversely affect its ability to forecast downslope windstorms. Hence, the Eta Model's surface winds have not been included in the initialization of the two-dimensional numerical model. A number of simple schemes for initializing the wind speeds between the surface and the first level in the Eta Model soundings were tested. These sensitivity tests indicated the strength of the resulting lee-slope flow can be sensitive to the method used to extend the Eta Model wind profile to the surface. Of the schemes considered, simply extending the wind speed at the first level in the Eta Model sounding down to the surface (i.e., a layer of constant wind speed) produced the best overall agreement between the two-dimensional model forecasts and the observed peak gusts for at least three of the locations considered in this study. All of the model forecasts presented here were obtained using this constant wind speed method for determining the surface wind speed.

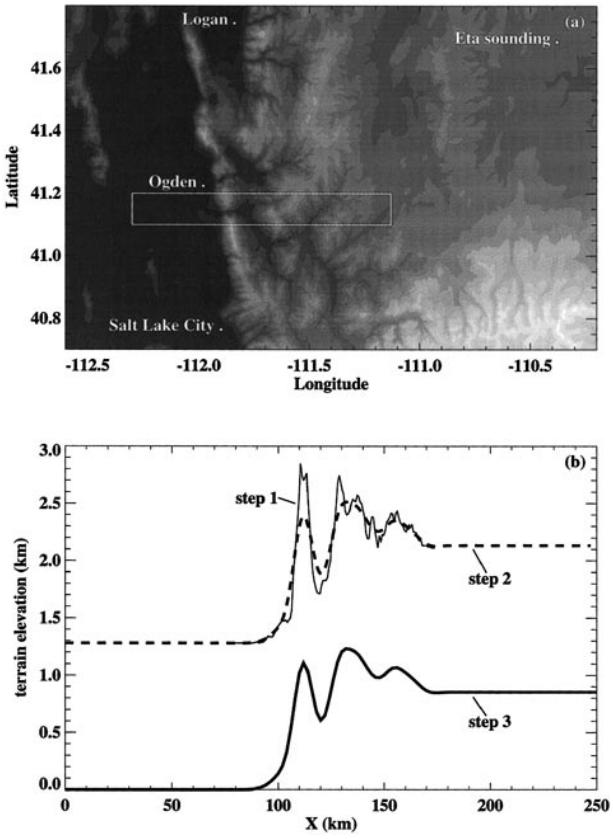


FIG. 1. (a) Gray shading plot of 30″ terrain elevation data for the Wasatch Front Range in northern Utah. Box indicates region used to derive representative terrain profile. (b) Line plot illustrating procedure used to derive each representative terrain profile. The thin solid line is the two-dimensional representation of the local terrain (step 1), the thick dashed line is the extended–smoothed terrain profile (step 2), and the thick solid line is the terrain profile that has been offset by a constant such that the minimum terrain elevation is zero (step 3).

The representative terrain profiles considered in this study are based on 30-s resolution terrain elevation data. Figure 1 illustrates the procedure used to derive each representative terrain profile. Each step of this procedure was carefully checked to assure all the profiles captured the overall two-dimensional character of the local terrain. The local terrain (boxed region in Fig. 1a) is collapsed to a single cross-barrier profile by retaining only the maximum terrain elevations along the direction parallel to the major ridge axis (thin solid line, Fig. 1b). The maximum terrain elevation is retained rather than averaging along the ridge to minimize the impact of smoothing on the overall height of the terrain. Level terrain is added to both ends of the resulting silhouette to reduce the influence of the lateral boundaries on the mountain wave solution. This extended profile is smoothed by applying a nine-point boxcar average three times. The smoothed terrain profile is then interpolated to the model grid using a cubic spline (thick dashed line, Fig. 1b). If the minimum terrain elevation of the

resulting terrain profile is nonzero, a constant is subtracted from the smoothed terrain profile such that the minimum terrain elevation is zero (thick solid line, Fig. 1b). Hence, the heights in the two-dimensional model are with respect to above ''ground level,'' where ground level refers to the minimum terrain elevation for the region under consideration. The geopotential heights associated with the upstream profile retrieved from the Eta forecast grid are with respect to mean sea level. To maintain the relationship between the underlying topography and the large-scale flow characteristics, the same constant is subtracted from the geopotential heights in the Eta profile. (That is, the geopotential heights are expressed in terms of heights above ground level.)

The direction of the horizontal wind vectors retrieved from the Eta gridded data will, for the most part, vary with height, whereas the two-dimensional model needs to be initialized with a unidirectional background flow. The projection angles considered in this study select the component of the large-scale flow perpendicular to the major axis of the local terrain. For example, the Wasatch Front Range in Utah, which is shown in Fig. 1a, lies from north to south such that a 90° wind is normal to the major axis of this mountain range. (That is, a projection angle of 90° was used in the Wasatch Front Range simulations.)

## 4. Historical high-wind events

The model's ability to capture past downslope windstorm events was investigated by generating numerical simulations for high-wind events that affected the following regions between January 1993 and April 1997: west of the Wasatch Front Range (Salt Lake City), west of the Washington Cascades (Enumclaw, WA), west of Salisbury Ridge (Juneau), northwest of the Chugach Range (Anchorage, AK), north of the Alaska Range (Delta Junction, AK), east of the Lewis Range (Great Falls, MT), and east of the Colorado Front Range (Boulder). These seven regions by no means represent an all-inclusive list of regions affected by downslope windstorms. This list simply indicates those forecast offices that participated in the study. The dates and observed wind speeds for the high-wind events considered in this study were provided by a representative from each respective forecast office. The model's performance was assessed by comparing the maximum surface wind speed within a specified region downstream of the model terrain at the final time of the numerical simulation with the observed lee-slope wind speeds (e.g., spotter reports, mesonet data).

The upstream profiles for these simulations were taken from the 12- or 18-h Eta Model forecasts valid at the time of the high-wind event. Prior to 12 October 1995, the Eta Model forecasts were generated using a horizontal grid spacing of 80 km and 38 layers in the vertical (Black et al. 1993). The Eta Model output was distributed to the local forecast offices on a grid with a horizontal spacing of 80 km, a vertical spacing of 50 mb, and a temporal spacing of 6 h. On 12 October 1995, the horizontal grid spacing in the Eta Model was reduced to 48 km (Rogers et al. 1996); however, the model fields were interpolated to the 80-km grid prior to distribution. The Eta soundings used in this study were retrieved from this distribution grid.

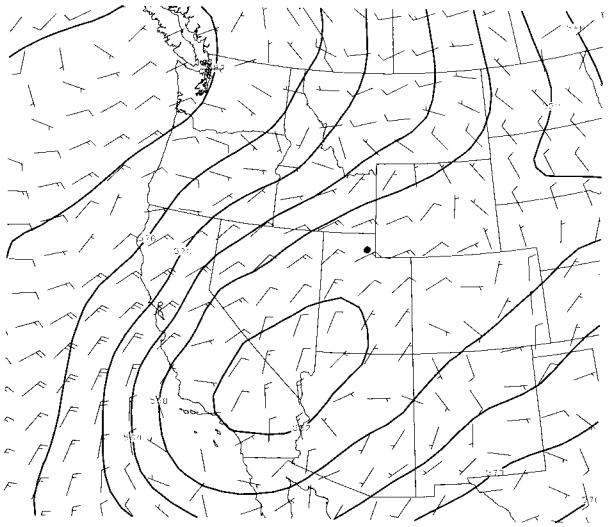

FIG. 2. The 500-mb heights and 850-mb winds valid 1200 UTC 24 Feb 1997. The location of the windstorm is identified with a large dot.

### *a. Case study: 24 February 1997*

In the early morning hours of 24 February 1997, damaging winds as strong as 36 m $s^{-1}$ (81 mph) struck the western slopes of the Wasatch Mountains in the general vicinity of Ogden, Utah (Fig. 1). Road and school closures, power outages, structural damage, and many downed trees were common across the area and accounted for several millions of dollars damage. Although the event was the severest to strike the area in nearly a decade, it typifies the local wave-induced windstorms observed in this area. In addition, it is the forecasting of this class of event that we hope will benefit from the tool being evaluated in this study.

Figure 2 shows the 500-mb heights and 850-mb winds from 1200 UTC 24 February. Of note is the upper-level trough located over extreme southwest Utah and southern Nevada that is in the process of retrograding south of the amplifying short-wave ridge evident to the north. This pattern places northeast Utah under relatively light 500-mb flow. The low-level circulation around the northern ridge (visible in the 850-mb wind field) is driving colder air south and west over the intermountain region. The superposition of these circulations induces strong easterly (cross barrier) low-level flow with decreasing easterly flow aloft. An inversion at the top of

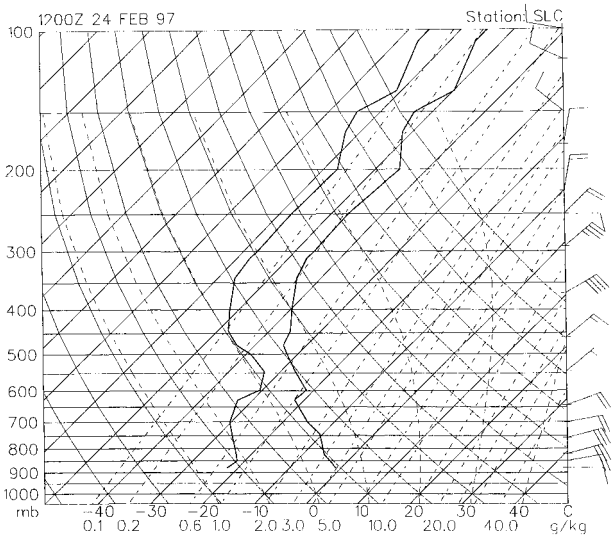


FIG. 3. Upper-air sounding from Salt Lake City airport at 1200 UTC 24 Feb 1997.

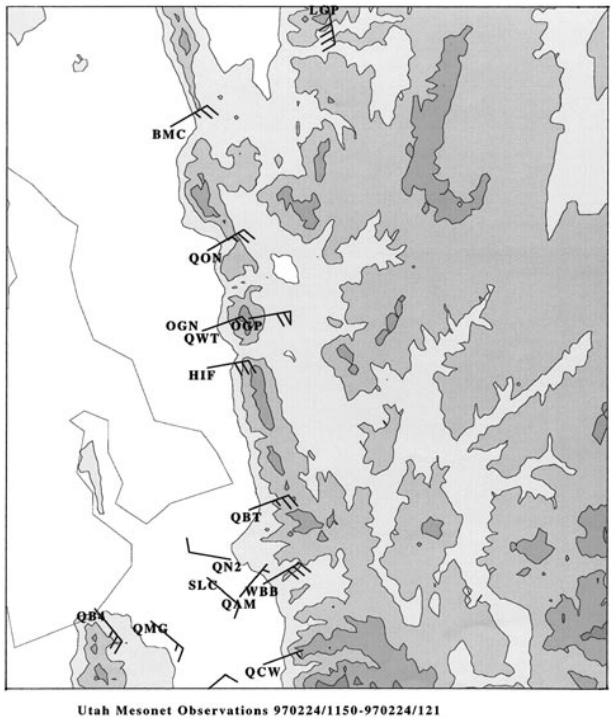


FIG. 4. Utah mesonet data in the vicinity of the Wasatch Mountains valid 1200 UTC 24 Feb 1997. Wind vector flags are 25 m $s^{-1}$, full barbs are 5 m $s^{-1}$, and half-barbs are 2.5 m $s^{-1}$. (Courtesy of University of Utah—J. Steenburgh).

the colder air mass is often associated with this circulation pattern. For this case, an inversion is evident at about 600 mb in the Salt Lake City sounding (Fig. 3) from 1200 UTC 24 February. Evidence of the stronger low-level flow is also apparent in this sounding. Given its downstream position from the Wasatch Front and the likelihood of conditions at this location being influenced by any related mountain wave activity, one must interpret this sounding with some caution. In other words, the Salt Lake City sounding is not necessarily representative of the ''undisturbed'' flow.

A collection of mesonet data (Fig. 4) taken during the windstorm reveals some of the challenges faced by forecasters in regions of complex terrain. The sharp north-to-south ridge is the Wasatch Front, the location of the strongest wave-induced winds in northern Utah. In addition to the sharpness of the ridge, the terrain contains pronounced gaps. Such breaks or gaps are common in complex terrain. Flow is accelerated through these gaps whenever there is a cross-barrier pressure gradient. Although typically lighter than the wave-induced winds, the pressure-gradient-driven gap winds, known locally as canyon winds, can be damaging. In many locations, gap winds are commonly observed during wave-induced windstorms and have resulted in local forecast rules placing greater emphasis on cross-barrier pressure gradients than is warranted for purely wave-induced storms. The 30 m $s^{-1}$ wind speed on the summit of Ogden Peak (OGP) is suggestive of wave activity. However, it is difficult to determine which process is active from the 15 m $s^{-1}$ observation at Hill Air Force Base (HIF) alone. This notoriously windy location is exposed to both wave-induced and gap winds. Ogden (OGN) on the other hand is not impacted by gap flow and is impacted by wave-induced winds only when the strongly accelerated flow propagates down to the lower slopes of the mountains. Lack of penetration to the lower slopes likely explains why Ogden is only reporting 7.5 m $s^{-1}$ at this time. Another clue supporting wave activity at this time is several stations with variable winds (not shown) and a westerly component (e.g., QN2), which is indicative of overturning or rotors. The coexistence of these two terrain-induced phenomena has often resulted in confusion among forecasters as to which parameters are the best predictors. The tool presented here would allow forecasters to focus directly on one of the phenomena and ideally help differentiate between the two.

Although output from the forecast tool being investigated here was not available at the time of the event, retrospective model runs reveal encouraging results. A cross section of the forecast wind velocity along the transect shown in Fig. 1 is given in Fig. 5. This forecast was generated by initializing the two-dimensional model with an Eta Model 18-h forecast sounding valid at 1800 UTC 24 February 1997, which is very close to the peak of the windstorm. Note the classic wave structure with strong low-level acceleration; the model forecast maximum surface winds at this time were 34 m $s^{-1}$. If the tool presented here had been in use at the time of the event, this forecast would have been available to the forecasters at least 12 h before the onset of strong winds.

As the event unfolds over the preceding 24 h, the increase in cross-barrier flow is clearly evident (Fig. 6).

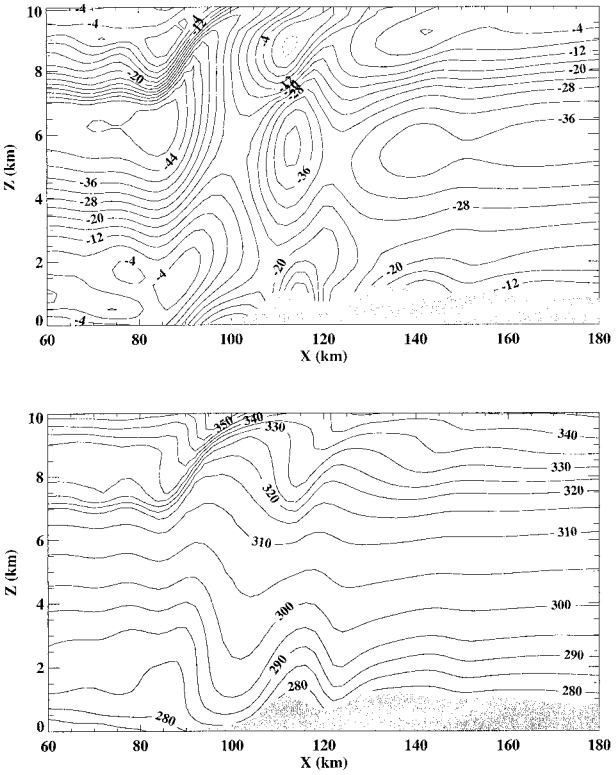


FIG. 5. (a) Horizontal wind speed (m $s^{-1}$) and (b) potential temperature fields from a two-dimensional model simulation initialized with an upstream sounding taken from the 18-h forecast of the 0000 UTC 24 Feb 1997 Eta Model run.

During this time period the magnitude of the cross-barrier flow in the Eta Model forecast (12- and 18-h forecasts) changes from near zero to values in excess of 30 m $s^{-1}$. The bold solid line in Fig. 6 corresponds to the wind profile used to generate the model output shown in Fig. 5. For all times, notice the strong decrease in cross-barrier flow with height above 7 km and the mean-state critical level above 10 km. The low-level inversion is also apparent in the profiles of potential temperature.

A time series of two-dimensional model forecast wind maxima generated from these wind and potential temperature profiles reveals notable skill (Fig. 7). For the time period between 0600 UTC 24 February and 0000 UTC 25 February, both the observations from the lower-elevation sites along the western slopes of the Wasatch Front Range (filled square, ■) and two-dimensional model forecasts (filled diamond, ♦) indicate wind speeds close to or exceeding the threshold for a High Wind Warning. Once again, the two-dimensional model forecasts would have been available to local forecasters 6–12 h before the onset of the strong winds.

### *b. Summary of results*

The results for the high-wind events that occurred along the western slopes of the Wasatch Front Range between January 1993 and April 1997 are summarized in Fig. 8. The date of each high-wind event is indicated along the horizontal axis. The square markers in Fig. 8 indicate the range of peak gusts reported during each high-wind event. These peak gust reports are from as far north as Logan and as far south as Salt Lake City (see Fig. 1a). The diamond markers indicate the two-dimensional model prediction for the time period corresponding to the observed maximum peak gust. The thick solid line demarcates the peak gust threshold for a High Wind Warning along the western slopes of the Wasatch Front Range [58 mph (26 m $s^{-1}$)]. The maximum lee-slope wind speeds from the two-dimensional simulations for this region fall within or slightly above the observed range of peak gusts for all but two events. For these two events, the model drastically underforecast the lee-slope flow.

The results for the high-wind events that occurred along the western slopes of the Washington Cascades (not shown) are very similar to those for the Wasatch Front Range. Both of these regions are also known to be affected by gap winds. Since gap flow is inherently three-dimensional, this particular tool cannot be expected to resolve gaptype high-wind events or high-wind events due to some type of interaction between these two types of terrain-induced flow. In postanalysis, it is particularly difficult, if not impossible, to determine which of these two mechanisms is responsible for the observed high winds due to the lack of high-resolution observational data. The high-wind events in these two regions for which the two-dimensional model drastically underforecast the lee-slope wind speeds may simply be cases in which gaptype flow played an important role. If these events were gaptype events, the model's ability to forecast mountain wave events in these two regions may be even better than that suggested by the test cases considered in this study.

The results for the high-wind events that occurred along the western slopes of Salisbury Ridge are summarized in Fig. 9a. The square markers indicate the magnitude of the maximum peak gust observed during each high-wind event. Most of these peak gust observations are from an automated weather station located at Sheep Creek. Additional observations are from Mayflower Island, the Juneau Federal Building, and the Juneau International Airport (see Fig. 10a). The bold solid line indicates the peak gust threshold for a High Wind Warning along the western slopes of Salisbury Ridge [58 mph (26 m $s^{-1}$)]. Although the two-dimensional model prediction is not necessarily a good indicator of the exact magnitude of the peak gusts associated with these high-wind events, the model is, for the most part, able to produce lee-slope wind speeds for these historical high-wind events that exceed the peak gust threshold for a High Wind Warning, especially during the more recent time period. The Eta Model has gone through several enhancements during this time period. Given that the accuracy of the forecast produced by the

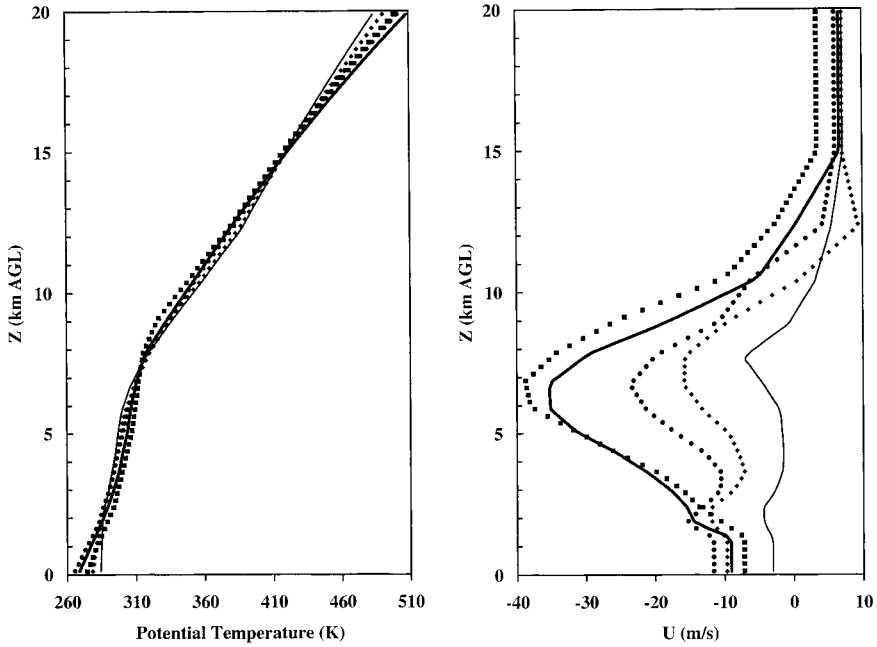


FIG. 6. Profiles of cross-barrier wind component and potential temperature taken from 12- and 18-h forecasts of three different Eta Model runs (97022312f12 = thin solid line; 97022312f18 = filled diamond, ♦; 97022400f12 = filled circle, ●; 97022400f18 = bold solid line; and 97022412f12 = filled square, ■) that show the evolution of the upstream flow conditions from 0000 UTC 24 Feb to 0000 UTC 25 Feb. Ground level zero corresponds to the elevation of Salt Lake City.

two-dimensional model is inherently dependent on how accurately the Eta Model predicts the characteristics of the large-scale flow, this trend in the two-dimensional model predictions may reflect improvements in the Eta Model forecast.

The results presented in Fig. 9a address only how well the two-dimensional model captures the maximum of each high-wind event, whereas the ability to predict the onset and duration of each wind event is also an important aspect of this forecast problem. The time series shown in Fig. 11 illustrate how the two-dimensional model performed with respect to the onset and duration of two Taku wind events: 12–16 February 1994 and 4–12 November 1995. The solid squares and circles represent the peak gusts recorded at Sheep Creek (over

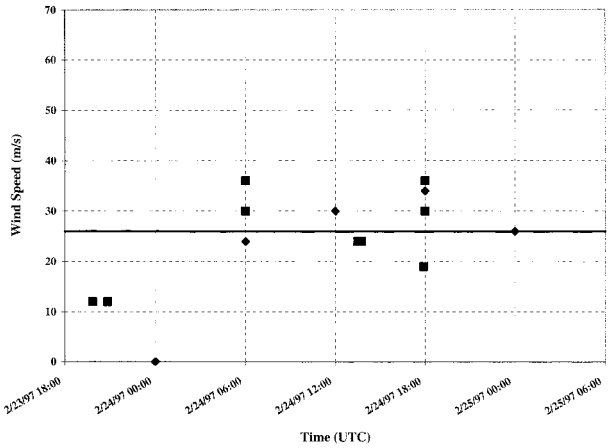


FIG. 7. Peak gust reports from lower elevation sites along the western slopes of the Wasatch Front Range (shaded square, ■) and the corresponding two-dimensional model predictions (filled diamond, ♦) for the high-wind event on 24 Feb 1997. Thick solid line demarcates the peak gust threshold for a high-wind warning along the western slopes of Wasatch Front Range.

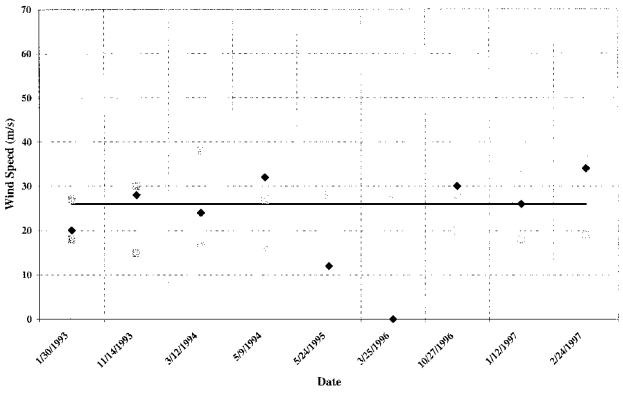


FIG. 8. Range of reported peak gusts for high-wind events that occurred along the western slopes of the Wasatch Front Range (shaded square, ■), and the two-dimensional model prediction for the time period corresponding to the observed maximum peak gust (filled diamond, ♦). The thick solid line demarcates the peak gust threshold for a high-wind warning along the western slopes of the Wasatch Front Range.

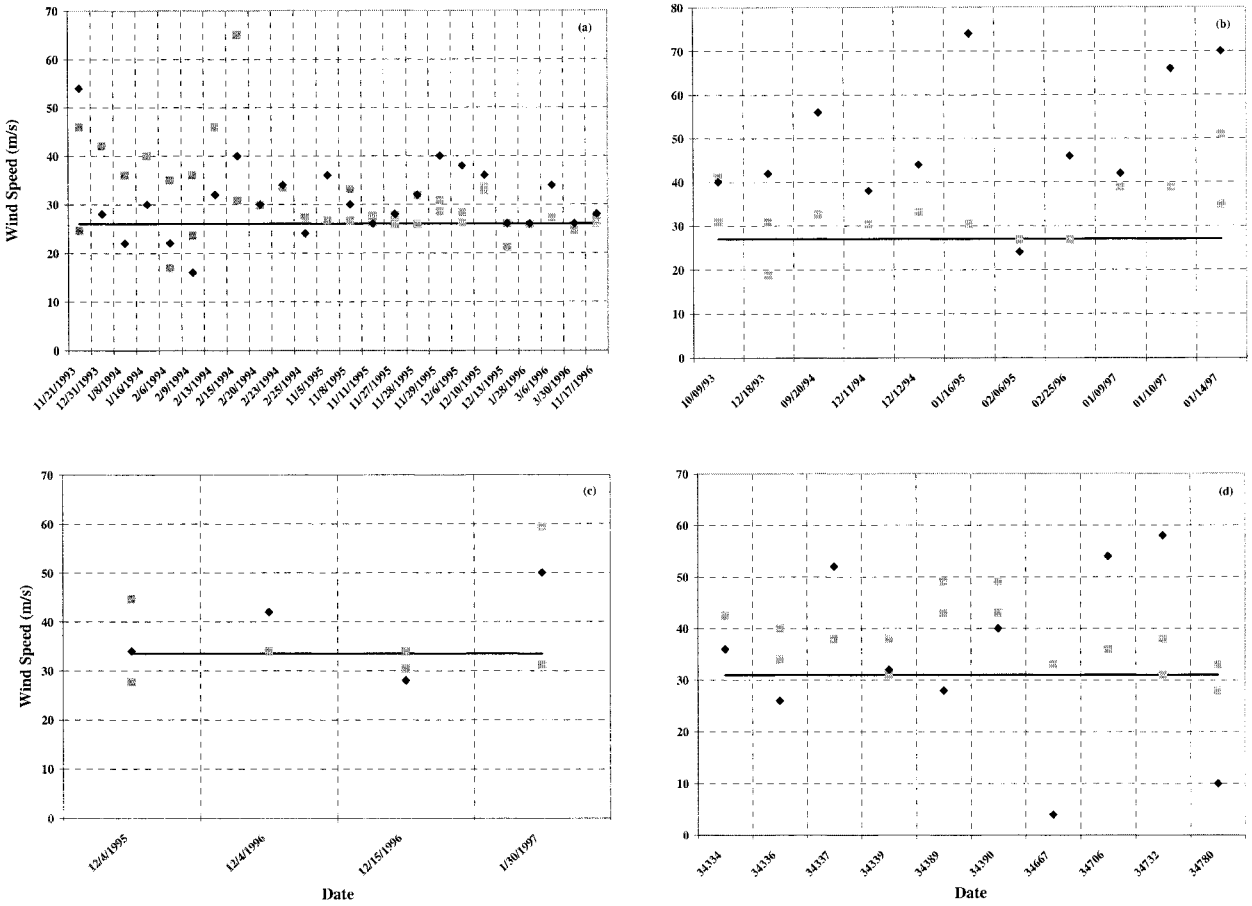


FIG. 9. Same as Fig. 8 except for the (a) western slopes of Salisbury Ridge, (b) northwestern slopes of the Chugach Range, (c) eastern slopes of the Lewis Range, and (d) eastern slopes of the Colorado Front Range.

1-h durations) and Mayflower Island, respectively, and the open squares represent instantaneous wind speeds recorded at Sheep Creek every hour.

The peak gusts associated with the 1994 event were rather strong (45–65 m $s^{-1}$) and exhibited two maxima: a primary maximum around 1800 UTC on 15 February and a secondary maximum around 1200 UTC on 13 February (Fig. 11a). For this particular event, the two-dimensional model was able to capture both the onset and the evolution of the windstorm.

The winds associated with the 1995 event were more moderate, only exceeding the peak gust threshold for relatively short time periods (Fig. 11b). The maximum observed peak gusts for this event agree fairly well with their corresponding model predictions (see Fig. 9a), but the model overforecast the longevity and, at times, the strength of the high winds. And yet, the observations shown in Fig. 11b represent the lee-slope flow at only two locations along the western slopes of Salisbury Ridge. Since the strength of the peak gusts associated with any particular downslope windstorm can exhibit large spatial variations, it is possible that the model predictions are more (or possibly less) representative of the overall behavior of the flow along the western slopes of Salisbury Ridge than the time series shown in Fig. 11b suggests.

The results for the high-wind events that occurred along the northwestern slopes of the Chugach Range are summarized in Fig. 9b. The observations for this location are mostly spotter reports from East Anchorage or the adjacent hillsides (see Fig. 10b). The predictions from the two-dimensional model generally met the peak gust threshold for a High Wind Warning in this region [60 mph (27 m $s^{-1}$)], but the model had a tendency to significantly overforecast the reported lee-slope wind speeds. The results for the high-wind events that occurred along the northern slopes of the Alaska Range (not shown) are very similar to those for the Chugach Range. Wind speed observations in the lee of the Chugach and Alaska Ranges are rather sparse. Hence, sampling limitations may be responsible for the two-dimensional model's tendency to significantly overforecast the wind speeds in these two regions.

Simulations for the high-wind events that occurred along the eastern slopes of the Lewis Range (Fig. 9c) produced lee-slope wind speeds that basically captured

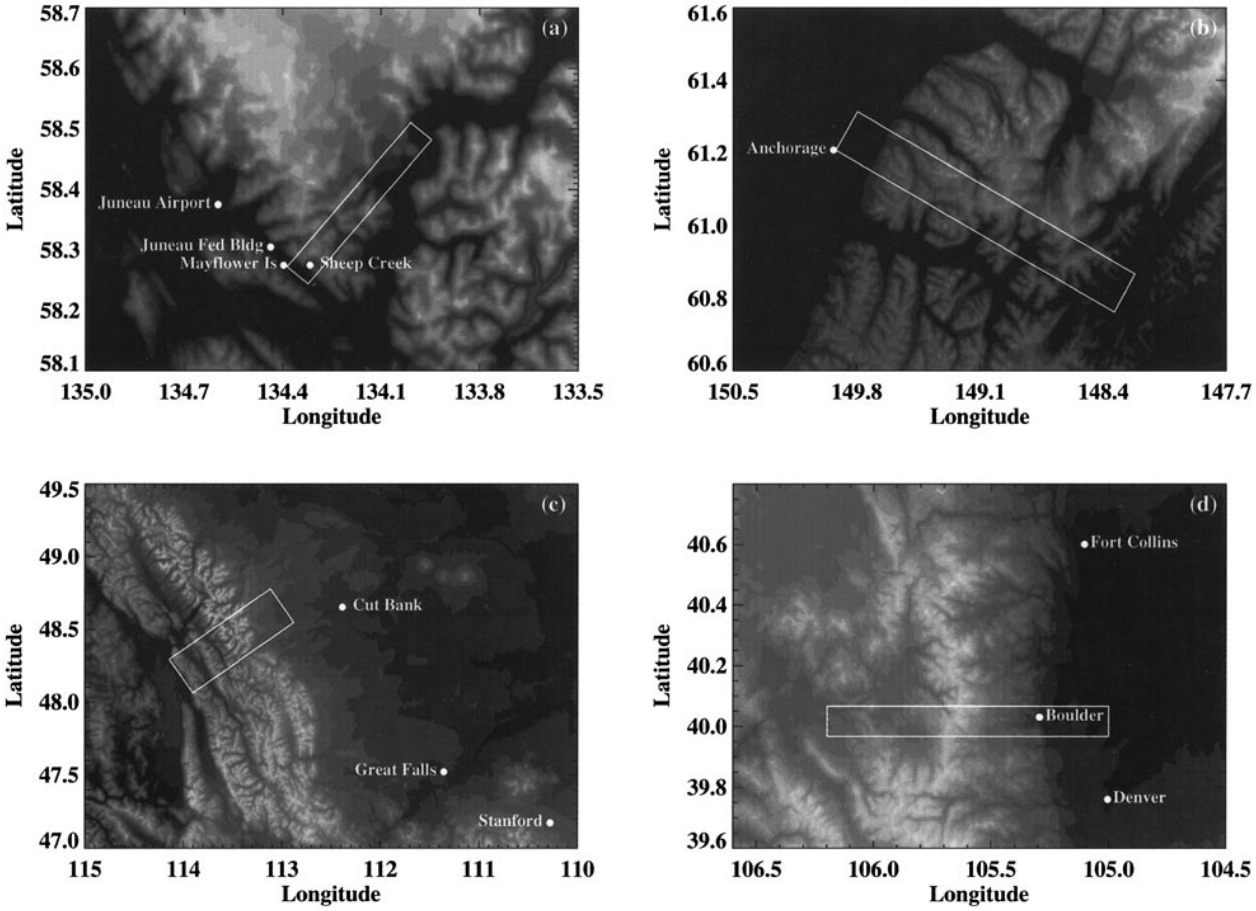


FIG. 10. Same as Fig. 1a except for (a) Salisbury Ridge, (b) Chugach Range, (c) Lewis Range, and (d) Colorado Front Range.

the strength of the peak gusts associated with each event. The peak gust reports for these high-wind events are from as far north as Cut Bank and as far south as Stanford (see Fig. 10c). On the other hand, four high-wind events is not a very thorough test of the model's ability to capture high-wind events in this particular region. This small number of events is by no means indicative of how often downslope windstorms affect this particular region. The Eta grids were simply missing from the data archive for a number of the high-wind events for which the representative from the Great Falls forecast office provided observational data.

The results for the high-wind events that occurred along the eastern slopes of the Colorado Front Range are summarized in Fig. 9d. The peak gust reports for these high-wind events are from as far north as Fort Collins and as far south as Denver (see Fig. 10d). The two-dimensional model generated lee-slope wind speeds that, for the most part, exceeded the peak gust threshold for this region [70 mph (31 m $s^{-1}$)], but the predictions that did meet the high-wind criterion were not necessarily a good indicator of the exact magnitude of the peak gusts associated with these high-wind events.

Although the two-dimensional model forecasts were not necessarily a good indicator of the exact magnitude of the observed peak gusts, the performance of this tool does look promising when viewed in terms of a threshold prediction, as shown in Fig. 12. The height of each stippled bar represents the percent of high-wind events for which the two-dimensional model generated lee-slope flow in excess of the local peak gust criterion. The numbers listed at the top of each bar represent the ratio of ''successful'' forecasts to the number of events considered at that location, otherwise know as the probability of detection. The success rates range from 50% along the western slopes of the Washington Cascades to 90% along the northern slopes of the Alaska Range. Two of the model predictions for the western slopes of the Wasatch Front (SLC), the location with the second lowest success rate, that are deemed unsuccessful under this criterion actually fall within the range of observed peak gusts (see Fig. 8; 30 Jan 1993 and 12 Mar 1994). The same is true for the western slopes of the Washington Cascades (SEA), the location with the lowest success rate. Since this prospective tool represents the windstorm as a single two-dimensional slice, one might expect its prediction to represent some intermediate solution to the extremes in the actual lee-slope flow. In

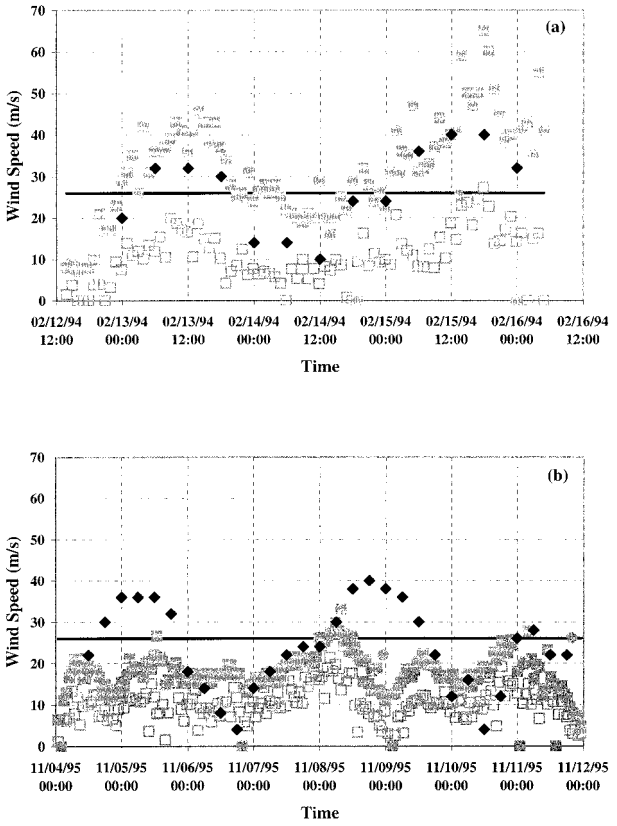


FIG. 11. Time series of instantaneous wind speeds recorded at Sheep Creek (open square, □), peak gusts recorded at Sheep Creek (shaded square, ■) and Mayflower Island (shaded circle, ●), and the corresponding two-dimensional model predictions (filled diamonds, ♦) for the Taku events on (a) 12–16 Feb 1994 and (b) 4–12 Nov 1995. Thick solid line demarcates the peak gust threshold for a High Wind Warning along the western slopes of Salisbury Ridge.

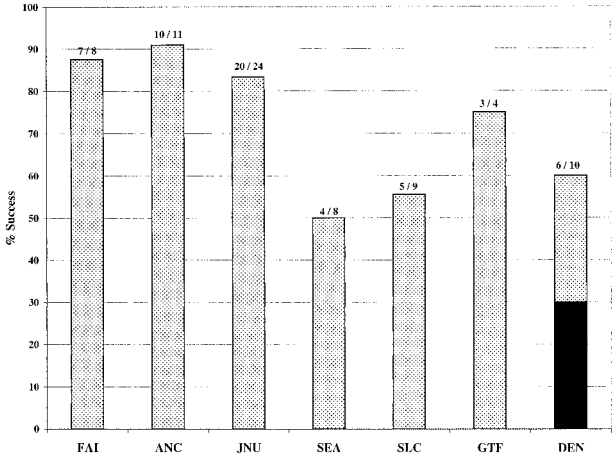


FIG. 12. Bar graph illustrating performance of two-dimensional model in terms of a threshold prediction. The height of each stippled bar represents the percent of high-wind events for which the two-dimensional model generated lee-slope flow in excess of the peak gust criterion for that particular location (FAI = northern slopes of the Alaska Range, ANC = northwestern slopes of the Chugach Range, JNU = western slopes of Salisbury Ridge, SEA = western slopes of the Washington Cascades, SLC = western slopes of the Wasatch Front Range, GTF = eastern slopes of the Lewis Range, and DEN = eastern slopes of the Colorado Front Range). The numbers listed at the top of each bar represent the ratio of successful forecasts to the number of events considered at that location. The height of the solid bar indicates the percent of Colorado Front Range wind events for which the Denver forecast office issued a High Wind Watch.

this context, the performance of this tool in these two locations would be more promising than the statistics shown in Fig. 12.

Another important aspect of this potential tool's evaluation is how its performance compares with that of the current windstorm forecast technique. Information on whether or not a High Wind Watch was posted prior to the high wind events considered in this study was only available from the Denver NWSFO. The height of the solid bar in Fig. 12 indicates the percent of Colorado Front Range events for which the forecast office issued a High Wind Watch (30%). This comparison suggests that a forecast tool like the one considered in this study would be a definite improvement over the decision tree currently used by the Denver forecast office. One of the three High Wind Watches issued by the Denver NWSFO that was included in the statistics for the current forecast technique was actually taken down shortly before the winds began to increase. This case was included as a success for the current forecast technique because this turn of events was probably more indicative of the forecasters' lack of confidence in the decision tree, rather than the accuracy of the forecast tool itself.

### *c. Discussion*

The tendency of the two-dimensional model to significantly overpredict the lee-slope flow for some locations (e.g., northwest of the Chugach Range and north of the Alaska Range), while producing wind speeds in fairly good agreement with observations for other locations (e.g., west of the Wasatch Front and west of the Washington Cascades) proved to be an interesting result of this study. Given the regional differences in the upstream conditions associated with downslope windstorms (e.g., a mean-state critical level is commonly associated with Taku events, whereas static stability layering or a wave-induced critical level is generally thought to be the mechanism responsible for windstorms along the eastern slopes of the Colorado Front Range), the two-dimensional model forecasts were first categorized according to whether or not the initial conditions contained a mean-state critical level and then categorized according to the difference between the observed peak gusts and the corresponding model prediction (see Fig. 13a). When a range of peak gust observations was available, the minimum difference between the reported peak gusts and the model prediction was used to categorize the model forecast, unless the prediction fell

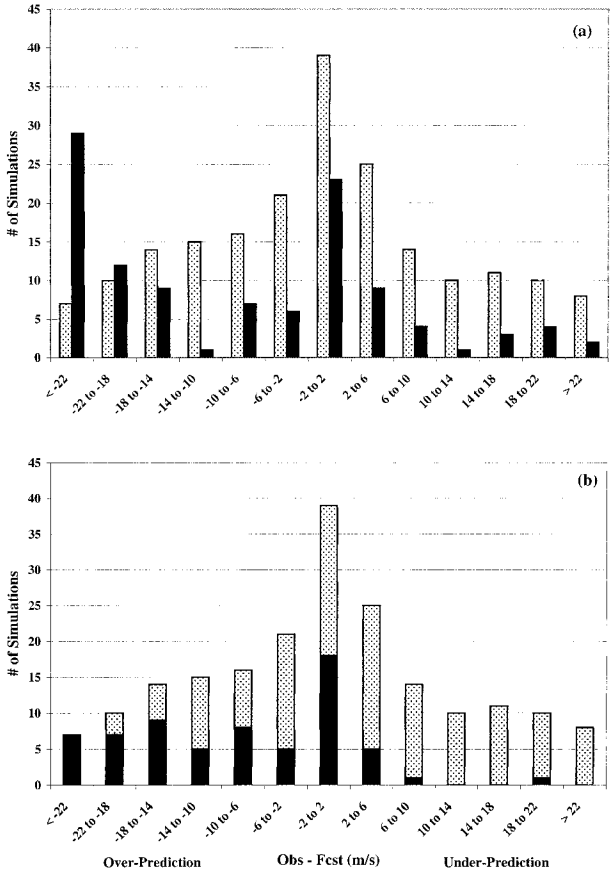


FIG. 13. (a) Bar graph partitioning the two-dimensional model predictions with respect to whether or not the initial conditions contained a mean-state critical level (stippled = mean-state critical level, solid = no mean-state critical level) and how the prediction compared with the observed peak gusts. (b) Bar graph partitioning the two-dimensional model predictions for initial conditions containing a mean-state critical level based on the height of the mean-state critical level (stippled = below 8 km; solid = above 8 km).

within the range of reported peak gusts. When the prediction fell within this range, the forecast was assigned to the −2 to 2 category. The mean-state critical level forecasts (stippled bars) have a distribution centered on the ''perfect'' forecast, the type of distribution one would desire. The no mean-state critical level forecasts (solid bars) have a bimodal distribution with a primary peak corresponding to large overpredictions and a secondary peak corresponding to the perfect forecast. These results suggest that the two-dimensional model tends to be overly active when static stability layering or a wave-induced critical level is the mechanism responsible for the low-level amplification of the mountain wave.

When the simulations for initial conditions with a mean-state critical level are subdivided with respect to the height of the mean-state critical level, where ''high'' refers to a critical level above 8 km and ''low'' refers to a critical level below 8 km, one finds that the simulations with a high mean-state critical level dominate the overprediction arm of the mean-state critical level distribution (see Fig. 13b). This tendency may stem from the fact that high-altitude mean-state critical levels are less likely to play an active role in the low-level amplification of a mountain wave than lower-level ones. In other words, static stability layering or a wave-induced critical level may actually be the mechanism responsible for the low-level amplification of the terrain-induced waves when the mean-state critical level is located above 8 km.

The performance of a forecast tool like the one considered in this study will be influenced by a number of factors. These factors can be grouped into three basic categories: 1) the initialization of the two-dimensional model, 2) the formulation of the two-dimensional model, and 3) the representativeness of the observations.

Consider first the initialization of the two-dimensional model. The value of guidance provided by mesoscale models, whether they are two- or three-dimensional, will be limited if the synoptic-scale forecast has significant errors. Variations in the accuracy of the synoptic-scale forecast could explain why the two-dimensional model is able to predict some high-wind events at a particular location, while failing miserably for other events. A bias in the large-scale forecast, such as under-(over-) forecasting the strength of the mountaintop inversion, could lead to the two-dimensional model being overly active when the upstream flow lacks a mean-state critical level. What is considered a significant error in the synoptic forecast will depend on the phenomenon one is trying to forecast. An important question this study has not addressed is the sensitivity of downslope windstorms to realistic uncertainties in the upstream stratification and wind profile. In other words, are further improvements in the accuracy of the larger-scale predictions necessary in order to achieve forecast skill beyond what is demonstrated in this study? In addition to the accuracy of the large-scale forecasts, the performance of this tool may depend on the temporal and vertical resolution of the soundings used to initialize the two-dimensional model. If a rather shallow inversion layer plays an important role in the low-level amplification of the mountain wave, then the 50-mb vertical spacing of the grids available to the forecast office may be too coarse to resolve this feature. If a high-wind event is rather short lived, then conditions conducive to achieving low-level amplification of the mountain wave may not be captured by the 6-h temporal resolution of the grids available to the forecast office.

A perfect prediction of the large-scale flow characteristics with the necessary temporal and spatial resolutions will not guarantee that a tool like the one considered in this study will produce a perfect forecast. The performance of this type of tool will also depend on how well the numerical model captures the behavior of this mesoscale phenomenon. Subtle features of the two-dimensional model considered in this study, such as the finite-difference schemes, boundary conditions, and

subgrid-scale parameterization, will affect the outcome of the numerical simulations, as well as the characteristics of the representative terrain profile and the method chosen for initializing the surface wind speed. Processes not represented in the tool's current configuration, such as boundary layer processes and the effects of moist processes, could also have a significant impact on the performance of this tool (Richard et al. 1989; Durran and Klemp 1982). Another factor that might impact this tool's performance are three-dimensional effects. Clark and Farley (1984) found that adding the along-ridge dimension to their simulations of the 11 January 1972 Boulder windstorm reduced the surface wave drag by approximately 20%. Recent work by Clark et al. (2000) showed that many aspects of the moderate 9 December 1992 Colorado downslope windstorm were inherently three-dimensional and are not represented in idealized models using two-dimensional dynamics. An inability of the two-dimensional framework to adequately represent the dynamics of self-induced critical levels may explain the model's tendency to be overly active when a mean-state critical level is not present in the upstream flow. Unless it can be established that three-dimensional dynamics are fundamental to most downslope windstorms, our idealized two-dimensional framework should still be able to provide much needed guidance for downslope windstorm forecasting.

The availability of observations can also impact the ''apparent'' performance of a forecast tool like the one considered in this study. As noted earlier, the strength of the peak gusts associated with a particular downslope windstorm can exhibit large spatial variations. Hence, observations from only one or two locations along the lee slope may not be representative of the overall strength of a particular windstorm. The sparsity of observations can also limit one's ability to determine the mechanism (downslope vs gap) responsible for a particular terrain-induced high-wind event. Since gaptype events are inherently three-dimensional, the inclusion of this type of event in the evaluation of a tool like the one considered in this study would misrepresent this forecast tool's ability to predict mountain wave high-wind events.

## 5. Plans for further evaluation

The results presented suggest a nonlinear two-dimensional mesoscale model initialized with vertical profiles taken from a larger-scale weather prediction model can, for the most part, produce lee-slope wind speeds that meet the high-wind criterion on those dates for which high winds are observed. On the other hand, these test cases do not address how well the model performs during nonwindstorm events (the null case). The two-dimensional model performed perfectly for two potential false warning cases provided by the Salt Lake City NWSFO, whereas a preliminary test of the model's ability to differentiate between windstorm and nonwindstorm events along the eastern slopes of the Colorado Front Range during the winter of 1996/97 suggests the false warning rate for this tool may be high, at least when applied to this particular region. Downslope windstorms along the eastern slopes of the Colorado Front Range tend to be associated with static stability layering and wave-induced critical levels. A high false warning rate for this region could be the result of the two-dimensional model's tendency to be overly active under these conditions. A surface inversion was present in 88% of the Denver soundings corresponding to these ''false warnings.'' The work of Lee et al. (1989) suggests the inability of the current two-dimensional model configuration to account for the presence of a cold pool downstream of the mountain ridge could also be responsible for this high false warning rate. The influence of a cold pool downstream of the mountain ridge would also be of concern along the lee slopes of the Alaska, Chugach, and Lewis Ranges. If the influence of cold pools in the lee of the mountain ridge proves to be a problem in these regions, modifying the initialization of the two-dimensional model or combining the model output with a decision tree that directs the forecaster to consider the conditions downstream of the mountain ridge may be able to reduce the false warning rate for these regions to an acceptable level.

As the preliminary tests for the Colorado Front Range demonstrated, consideration of the null case is an important part of the evaluation of this tool's ability to forecast downslope windstorms. Hence, further testing of this tool is ongoing and will continue through the winter months of 2000/01. During this evaluation period, the model will be run locally in real time on a workstation in the Fairbanks, Anchorage, Juneau, Seattle, Salt Lake City, Great Falls, and possibly Denver (now located in Boulder) forecast offices. A representative from each office is in charge of evaluating this tool's performance in their respective region. Direct involvement by the operational forecasters may prove to be important to the ultimate success of this forecast tool because the forecasters will be able to provide important insights into the conditions in their local region. Such insights may lead to improvements in the model configuration.

## 6. Summary

High-wind events resulting from the low-level amplification of terrain-induced gravity waves are a major concern to operational forecasters whose area of responsibility contains significant terrain features. The winds associated with this mesoscale phenomenon can gust to well above nominal hurricane force and are usually highly variable in both space and time. The family of weather prediction models currently run at NCEP are not able to explicitly predict downslope windstorms. Current windstorm forecast techniques commonly utilize decision trees to assess the probability of high winds

due to this mesoscale phenomenon, a technique operational forecasters have not found to be highly reliable when forecasting downslope windstorms. This study looked at a new tool that may be able to improve the accuracy of downslope windstorm forecasts: a two-dimensional, nonlinear, mesoscale numerical model, initialized with upstream profiles taken from Eta forecast grids, run in real time on a workstation in the local forecast office.

Numerical simulations for historical high-wind events that affected seven regions in the United States between January 1993 and April 1997 indicate this tool is able to produce lee-slope wind speeds that meet the local peak gust threshold for a High Wind Warning for a majority of those cases (50%–90%) where the observed winds met this threshold. The number of ''successful'' forecasts increases if events for which the lee-slope wind speeds in the two-dimensional simulations did not meet the peak gust threshold but did fall within the range of observed peak gusts are considered successful forecasts (75%–90%). A comparison between the High Wind Watches posted for the historical Colorado Front Range high-wind events and the two-dimensional model forecasts suggests that this new tool would be a definite improvement over the current forecast technique (success rate would have increased from 30% to 60%).

Probably the most intriguing result of this study is the tendency of the two-dimensional model to significantly overpredict the lee-slope flow in some locations, while producing wind speeds in fairly good agreement with observations in other locations. This trend is apparently connected to regional variations in the prevalent mechanism for the low-level amplification of the terrain-induced waves. The tendency of the two-dimensional model to be overly active when static stability layering or a wave-induced critical level is the mechanism responsible for the low-level amplification of the mountain wave may be related to problems with the initial conditions (i.e., the ability of the Eta Model to accurately forecast the relevant features of the flow), or an inability of the two-dimensional model to adequately represent the dynamics of self-induced critical levels.

When evaluating a tool like the one presented here, where the phenomenon it is trying to predict is highly variable in both space and time, it is important to keep in mind that the temporal and spatial resolution of wind speed observations is generally rather poor, especially in sparsely populated regions like the northern slopes of the Alaska Range. These limitations make it difficult to thoroughly assess the performance of this forecast tool. In other words, the two-dimensional model may be doing a better (or possibly worse) job of representing the average behavior of the peak gusts along the lee slopes than is indicated by the available observations.

The test cases presented in this study evaluated how this new tool performed during high-wind events. Its performance during nonwindstorm events (null case) will play a very important role in its evaluation overall. A false warning can be as detrimental to the accuracy of a forecast tool as a missed event. Hence, further testing is on going and will continue through the winter months of 2000/01. During this time period, the two-dimensional model will be run locally in real time on a workstation in the Fairbanks, Anchorage, Juneau, Seattle, Salt Lake City, Great Falls, and possibly Denver (now located in Boulder) forecast offices. A preliminary test of the two-dimensional model's ability to differentiate between windstorm and nonwindstorm events along the eastern slopes of the Colorado Front Range suggests the false warning rate associated with this tool may be high for at least some of the regions affected by downslope windstorms. If this tendency is not related to limitations of the two-dimensional framework, modifications to the current configuration of this tool may be able to reduce the false warning rate to an acceptable level.

*Acknowledgments.* This research was supported by an appointment to the COMET Fellowship Program sponsored by the National Weather Service and administered by the University Corporation for Atmospheric Research under a Cooperative Agreement with the National Oceanic and Atmospheric Administration (NOAA Awards NA37WD0018-01 or NA67WD0097). Part of this work was performed while the first author held a National Research Council–NOAA/ETL Research Associateship. The authors would like to thank the following people for the information they provided on the high-wind events considered in this study: David Bernhardt, Bob Clay, Carl Dierking, Larry Dunn, Eric Stevens, and Eric Thaler. The authors would also like to thank Ernie Recker of the University of Washington for providing the archived Eta grids used in this study, Scott Jacobs of NCEP for his assistance in creating GEMPAK files, Dave Storm of NWSFO/Seattle for his assistance with computer related matters, Jim Steenburgh of the University of Utah for providing the figure for the Utah mesonet, and John Brown of NOAA/FSL for providing insightful feedback throughout this project.

## REFERENCES

Bergen, W. R., and A. H. Murphy, 1978: Potential economic and social value of short-range forecasts of Boulder windstorms. *Bull. Amer. Meteor. Soc.*, **59,** 29–44.

Black, T. L., D. G. Deaven, and G. J. DiMego, 1993: The step-mountain eta-coordinate model: 80 km ''early'' version and objective verifications. NWS Tech. Procedures Bull. 412, National Oceanic and Atmospheric Administration/National Weather Service, 31 pp. [Available from National Weather Service, Office of Meteorology, 1325 East–West Highway, Silver Spring, MD 20910.]

Brinkmann, W. A. R., 1974: Strong downslope winds at Boulder, Colorado. *Mon. Wea. Rev.*, **102,** 592–602.

Brown, J. M., 1986: A decision tree for forecasting downslope winds in Colorado. Preprints, *11th Conf. on Weather Forecasting and Analysis,* Kansas City, MO, Amer. Meteor. Soc., 83–88.

——, A. A. Rockwood, J. F. Weaver, B. D. Jamison, and R. Holmes, 1992: An expert system for the prediction of downslope wind-

storms. *Proc. Fourth Workshop on Operational Meteorology*, Whistler, BC, Canada, Atmospheric Environmental Service and Canadian Meteorological and Oceanographic Society, 352–357.

Clark, T. L., and W. R. Peltier, 1977: On the evolution and stability of finite-amplitude mountain waves. *J. Atmos. Sci.,* **34,** 1715–1730.

——, and R. D. Farley, 1984: Severe downslope windstorm calculations in two and three dimensions using anelastic interactive grid nesting: A possible mechanism for gustiness. *J. Atmos. Sci.,* **41,** 329–350.

——, W. D. Hall, R. M. Kerr, D. Middleton, L. Radke, F. M. Ralph, P. J. Neiman, and D. Levinson, 2000: On the origins of aircraft damaging clear-air turbulence during the 9 December 1992 Colorado downslope windstorm: Numerical simulations and comparison with observations. *J. Atmos. Sci.,* **57,** 1105–1131.

Colman, B. R., and C. F. Dierking, 1992: The Taku wind of southeast Alaska: Its identification and prediction. *Wea. Forecasting,* **7,** 49–64.

Durran, D. R., 1986: Another look at downslope windstorms. Part I: On the development of analogs to supercritical flow in an infinitely deep, continuously stratified fluid. *J. Atmos. Sci.,* **43,** 2527–2543.

——, 1990: Mountain waves and downslope windstorms. *Atmospheric Processes over Complex Terrain, Meteor. Monogr.,* No. 45, Amer. Meteor. Soc., 59–81.

——, and J. B. Klemp, 1982: The effects of moisture on trapped mountain lee waves. *J. Atmos. Sci.,* **39,** 2490–2506.

——, and ——, 1983: A compressible model for the simulation of moist mountain waves. *Mon. Wea. Rev.,* **111,** 2341–2361.

——, and ——, 1987: Another look at downslope windstorms. Part II: Nonlinear amplification beneath wave-overturning layers. *J. Atmos. Sci.,* **44,** 3402–3412.

——, M. Yang, D. N. Slinn, and R. G. Brown, 1993: Toward more accurate wave permeable boundary conditions. *Mon. Wea. Rev.,* **121,** 604–620.

Klemp, J. B., and D. K. Lilly, 1975: The dynamics of wave induced downslope winds. *J. Atmos. Sci.,* **32,** 320–339.

——, and D. R. Durran, 1983: An upper boundary condition permitting internal gravity wave radiation in numerical mesoscale models. *Mon. Wea. Rev.,* **111,** 430–444.

Lee, T. J., R. A. Pielke, R. C. Kessler, and J. Weaver, 1989: Influence of cold pools downstream of mountain barriers on downslope winds and flushing. *Mon. Wea. Rev.,* **117,** 2041–2058.

Lilly, D. K., and E. J. Zipser, 1972: The Front Range windstorm of 11 January 1972—A meteorological narrative. *Weatherwise,* **25** (2), 56–63.

Mass, C. F., and Y.-H. Kuo, 1998: Regional real-time numerical weather prediction: Current status and future potential. *Bull. Amer. Meteor. Soc.,* **79,** 253–263.

Ralph, F. M., P. J. Neiman, and D. Levinson, 1997: Lidar observations of a breaking mountain wave associated with extreme turbulence. *Geophys. Res. Lett.,* **24,** 663–666.

Reed, R. J., 1981: Case study of a bora-like windstorm in western Washington. *Mon. Wea. Rev.,* **109,** 2383–2393.

Richard, E., P. Mascart, and E. C. Nickerson, 1989: Role of surface friction in downslope windstorms. *J. Appl. Meteor.,* **28,** 241–251.

Rogers, E., T. L. Black, D. G. Deaven, and G. J. DiMego, 1996: Changes to the operational ''early'' eta analysis/forecast system at the National Centers for Environmental Prediction. *Wea. Forecasting,* **11,** 391–413.

Smith, R. B., 1985: On severe downslope winds. *J. Atmos. Sci.,* **42,** 2597–2603.

——, 1987: Aerial observations of the Yugoslavian bora. *J. Atmos. Sci.,* **44,** 269–297.

Staudenmaier, M., and J. Mittelstadt, 1997: Results of the Western Region evaluation of the Eta-10 model. Western Region Technical Attachment 97-18, 12 pp. [Available from National Weather Service, Scientific Services Division, 125 South State St., Salt Lake City, UT 84138-1102; available online at http://www.wrh.noaa.gov/wrhq/97TAs/TA9718/TA97-18.html.]